CHEMISTRY
A EUROPEAN JOURNAL

ChemPubSoc
Europe

DOI: 10.1002/chem.201200107

One-Pot Synthesized DNA–CdTe Quantum Dots Applied in a Biosensor for the Detection of Sequence-Specific Oligonucleotides

Cuiling Zhang, Jing Xu, Shiming Zhang, Xinghu Ji, and Zhike He*[a]

In the past decade, as a new class of fluorescent probes, semiconductor quantum dots (QDs) have been widely applied in the area of biosensing, immunoassays, and biological imaging because of their unique optical characteristics and biocompatibility.[1] In these applications, a number of biomolecule-labeled QDs were devoted to biospecific interactions, such as DNA-labeled QDs. These QDs can be usually used as a donor for molecular recognition mainly in fluorescence resonance energy transfer (FRET).[2] The coupling reaction between streptavidin QDs and biotin–DNA is a common approach for DNA-labeled QDs for the streptavidin–biotin specific reaction.[3] The method is convenient, but it has no advantage in FRET application, due to increasing the distance between the donor (the large size of the QD) and the acceptor. Furthermore, streptavidin QDs are expensive. DNA covalent bonding to QDs by reaction between the carboxy/amino group of QDs and amino/carboxy group modified DNA could overcome these flaws;[4] however; the acidic coupling conditions may lead to the breakdown of the QDs, which limits its application. Zhou et al. directly coupled a dye-labeled DNA acceptor to a QD donor through a thiol linker.[5] This method costs less, significantly reduces the donor–acceptor distance to increase the FRET efficiency, and at the same time retains the stability of the QDs . However, the process is multistep and complicated. A one-step synthesis of DNA-labeled QDs has been established in such an environment.[6] Phosphorothiolate phosphate (ps–po) DNA compounds were used as ligands to obtain DNA-labeled QDs. Herein, we have synthesized nucleic acid functionalized CdTe nanocrystals with different emission wavelengths by a one-step synthesis.

Recently, new emerging zero-bandgap carbon nanomaterials, graphene, and graphene oxide (GO) have attracted great interest in the fields of biology, chemistry, physics, and materials.[7] Graphene and GO have π-systems, which allows them very easily to accept electrons. Inspired by the property, researchers have used graphene and GO as energy acceptors to develop many biosensors based on the FRET system.[8] Importantly, graphene and GO possess a superquenching ability that is critical for the sensitivity of assays.[9] In addition, graphene displays better conductivity than GO, because GO has many oxygen-containing groups, which destroy the conjugate structure.[10] Thus, graphene was chosen as the energy acceptor in this paper. A biosensor, which is based on FRET from the DNA-functionalized CdTe nanocrystals to graphene, has been developed, that is, DNA–CdTe QDs prepared by a one-pot method, and its successful application in the analytical detection of the hepatitis B virus (HBV) surface–antigen gene is described for the first time.

Scheme 1 shows the preparation of DNA–CdTe QDs by a one-pot method.[6] Glutathione (GSH) and a specific-sequence DNA were used as a co-ligands to stabilize the QDs. The DNA ligand consisted of two domains: phosphorothiolates (sulfur-containing variants of the usual phosphodiester backbone), which preferentially bind to the CdTe surface over phosphates;[11] and a DNA-targeting area, which recognizes a certain molecule or protein. Then, the DNA–CdTe QDs were used in the analytical detection of HBV oligonucleotides. This biosensing platform was constructed according to the different adsorption properties of graphene towards single-stranded (ss)DNA compared with that of double-stranded (ds)DNA. The bases of the ssDNA are uncoiled partially and can be exposed to graphene. Thus, the strong π–π stacking of graphene with the bases and aromatic compounds in the ssDNA is presented. However, the formation of dsDNA reduces the exposure of the bases, which weakens the π–π stacking interaction.[12] Similar, behavior in this respect is also shown for gold nanoparticles. The expo-

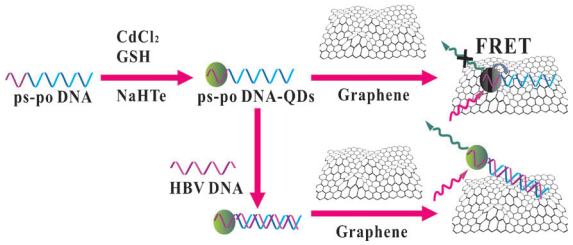

Scheme 1. A schematic illustration of the HBV-oligonucleotide detection with one-step synthesis DNA–CdTe as the energy donor and graphene as acceptor.

[a] C. Zhang, J. Xu, S. Zhang, X. Ji, Prof. Z. He
Key Laboratory of Analytical Chemistry
for Biology and Medicine (Ministry of Education)
College of Chemistry and Molecular Sciences
Wuhan University, Wuhan 430072 (P.R. China)
Fax: (+86) 27-68754067
E-mail: zhkhe@whu.edu.cn

Supporting information for this article is available on the WWW under http://dx.doi.org/10.1002/chem.201200107.

sure of bases causes the ssDNA to stick to the gold nanoparticles, which is attributed to the attractive van der Waals forces between the bases and the gold nanoparticle. But the dsDNA does not permit the uncoiling needed to expose the bases and always presents the negatively charged phosphate backbone of the oligonucleotide. Therefore, the repulsion between the negatively charged phosphate backbone and the citrate ions dominates the electrostatic interaction between the dsDNA and gold nanoparticles.[13] The detection of HBV DNA was realized in two steps: 1) QD-labeled ssDNA was hybridized with various concentrations of its target, resulting in the formation of dsDNA; 2) graphene was added into the above-mentioned mixture. It is anticipated that the fluorescence of the unhybridized ssDNA probe is effectively quenched by graphene, while the fluorescence of the hybridized dsDNA probe is maintained. It should be noted that the detection platform based on high DNA-binding specificity needs neither labeled QDs nor labeled graphene.

To realize such a design, we have synthesized DNA–CdTe QDs by a one-pot method, and the combination of DNA with CdTe was confirmed by UV/Vis absorption spectra (see Figure S1 in the Supporting Information). The typical absorption peak of DNA is observed at $\lambda = 260$ nm. Moreover, the normalized fluorescence spectra of CdTe QDs (GSH as the ligand alone) and DNA–CdTe QDs suggest that the spectrum of the latter is blueshifted under the same synthesis conditions (see Figure S2 in the Supporting Information). The quantum yield of the DNA–CdTe QDs is up to 20%, higher than that of CdTe QDs (13%, emission peak $\lambda_{em} =$ 528 nm). This phenomenon is attributed to the formation of a co-ligand containing GSH and DNA, which can offset the surface defect of CdTe QDs. QDs with different emission wavelengths were also obtained by simply changing the reaction time. The properties were characterized by UV/Vis absorption spectra (Figure 1A), in which the absorption around $\lambda = 260$ nm is clearly due to the DNA binding to QDs. The optical properties of the DNA–CdTe QDs are summarized as follows (Figure 1B): The emission peaks of DNA–CdTe QDs shift from $\lambda_{em} = 513$ to 584 nm, and the full width at half maximum (FWHM) increases from $\lambda = 39$ to 55 nm with the increase of reaction time from 40 min to 7.5 h. Furthermore, the typical TEM images for the as-prepared CdTe QDs and DNA–CdTe QDs are depicted in Figure S3 in the Supporting Information. From the TEM images, the dispersion ability of DNA–CdTe QDs is better than that of CdTe QDs. Thus confirming that DNA–CdTe QDs had been successfully prepared.

Graphene has been prepared by annealing GO synthesized by a modified Hummers' method.[14] However, graphene is difficult to dissolve in water because it is hydrophobic. A relatively stable suspension was prepared by mixing aqueous sodium dodecyl benzene sulfonate (SDBS; 0.02 wt%) with graphene in water by ultrasonication for 1 h. GO was characterized by AFM analysis (see Figure S4A in the Supporting information). The AFM image showed that the thickness of the as-synthesized GO sheets was about

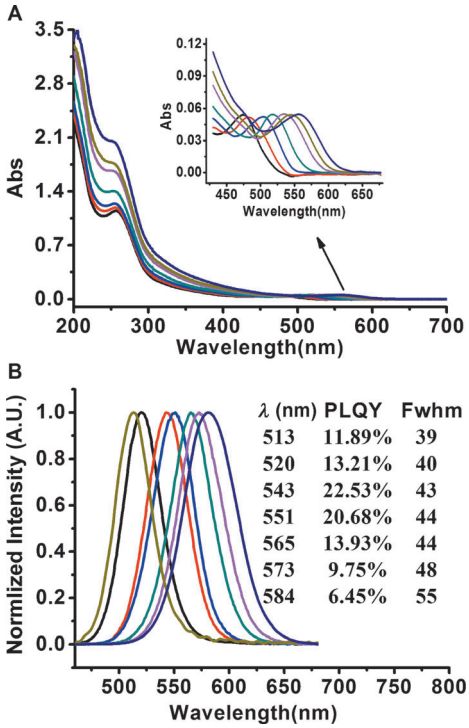

Figure 1. A) UV/Vis absorption. B) Fluorescence spectra of DNA–CdTe prepared at various reaction times (40 min, 1 h, 2.5 h, 3.5 h, 5 h, 6 h, and 7.5 h) with a series of maximum emission wavelengths. Related QY and FWHM values are presented ($\lambda_{ex} = 350$ nm).

1.3 nm. Taking the oxygen-containing group into account, the thickness is appropriate for single-layer GO. Figure S4B in the Supporting Information shows the TEM image of graphene obtained from the GO. The optical image in the inset shows that the SDBS–graphene is well dispersed in aqueous solution at a concentration of 0.25 mg mL^{-1} and is highly stable. Comparisons with the XRD and Raman spectra of graphite, GO, and graphene provided further evidence of the successful synthesis of graphene. As shown in Figure S5A in the Supporting Information, XRD data showed the characteristic diffraction peak of GO at $2\theta = 10.4°$, and the peak position increases after annealing, suggesting the decrease of interplanar spacing after thermal reduction.[15] The Raman spectrum displays the significant structural changes that occur during the chemical processing from graphite to GO and then to the graphene (Figure S5B in the Supporting Information). As expected, the spectrum of graphite is characterized by a strong band at $\tilde{\nu} \approx 1581$ cm^{-1} (G) and a weak band at $\tilde{\nu} \approx 1359$ cm^{-1} (D; $I_D/I_G = 0.26$). However, the D band of GO at $\tilde{\nu} \approx 1363$ cm^{-1} becomes prominent, and the G band is broadened and shifted to $\tilde{\nu} \approx 1594$ cm^{-1}, showing the reduction of the in-plane sp^2 domains, which is possibly attributed to the extensive oxidation. Clearly, the integrated intensity ratio of the D and G bands ($I_D/I_G = 1.52$) increases. After thermal annealing, the ratio of the intensities (I_D/I_G) increases to 1.66, although the reduced GO also contains both a G ($\tilde{\nu} \approx 1581$ cm^{-1}) and a D band ($\tilde{\nu} \approx 1352$ cm^{-1}). This phenomenon proves that the

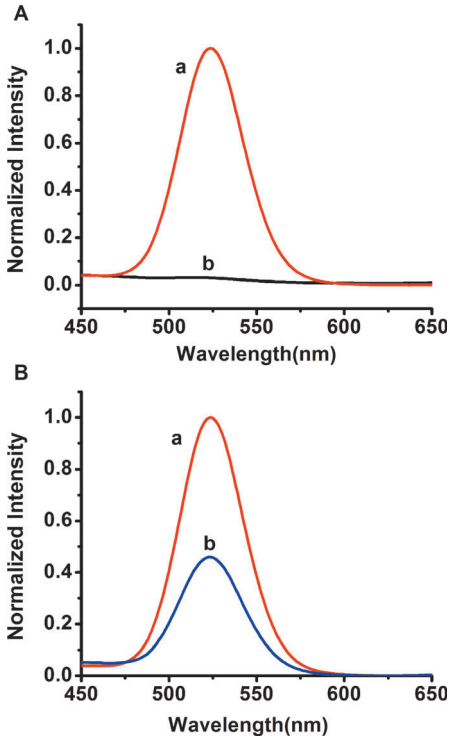

Figure 2. Fluorescence emission spectra of: A) DNA–QDs (25 nM); B) DNA–QDs incubated with target (800 nM) in Tris-HCl buffer (0.2 M, 150 mM NaCl, pH 7.4) a) before and b) after adding graphene (4 $\mu g\,mL^{-1}$) for 5 min.

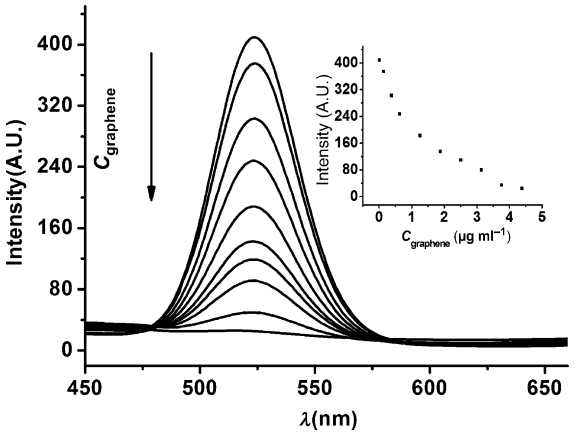

Figure 3. Fluorescence spectra of DNA–CdTe QDs in the presence of various concentrations of graphene in Tris-HCl buffer. Inset: fluorescent-intensity ratio versus concentration of graphene. DNA–CdTe QDs concentration = 25 nM; λ_{ex} = 350 nm.

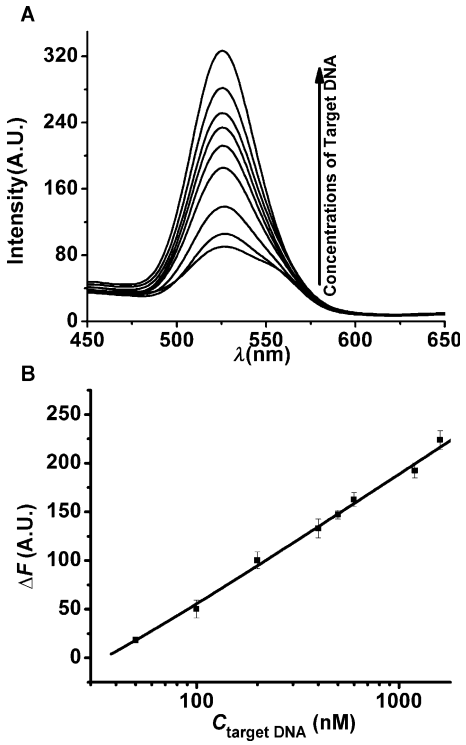

Figure 4. FRET-based hybridization assay for target HBV DNA. A) Fluorescence-emission spectra of the ssDNA–QDs after incubation with different concentrations of target HBV DNA (c = 50–2000 nM) for 10 min in Tris-HCl buffer (0.2 M, 150 mM NaCl, pH 7.4). B) The linear relationship between the increase of donor fluorescence and the logarithm value of target concentration within the range of 50 to 1600 nM (R = 0.9985).

carbon lattice of graphene returns to an essentially graphitic, but highly defected state.[16]

Furthermore, we investigated the different affinities of graphene on ssDNA and dsDNA (Figure 2). Upon addition of 4 $\mu g\,mL^{-1}$ graphene, ssDNA QDs showed a fluorescence quenching by more than 96% in 2-amino-2-hydroxymethyl-propane-1,3-diol buffer (Tris; Figure 2A), indicating the high-quenching efficiency of graphene. However, when ssDNA QDs were hybridized with the target to form dsDNA, the quenching efficiency became 54% (Figure 2B). The difference between the quenching efficiencies of graphene to ssDNA QDs and dsDNA QDs produced a method for sensing HBV DNA.

The energy transfer from DNA–CdTe QDs to graphene was studied as illustrated in the following experiment. The concentration of QDs was estimated by Peng's method.[17] As the concentration of grapheme increased, the fluorescence intensity of the DNA QDs (25 nM, in 0.2 M Tris-HCl buffer, pH 7.4, 150 mM NaCl) decreased (Figure 3) and trended to a minimum value at 4.375 $\mu g\,mL^{-1}$ (inset in Figure 3). However, as the concentration of complementary HBV DNA[18] applied to hybridization increased, the fluorescence intensity of QDs gradually increased (Figure 4A). According to the literature, that should be attributed to the formation of dsDNA between the capture DNA and the target DNA, which would reduce the exposure of the base, then impair the noncovalent π–π stacking interaction and hydrogen-bonding interactions. Thus, the distance between the CdTe and graphene increased, leading to a considerable reduction in the efficiency of FRET.[12] The fluorescence recovery value ΔF ($\Delta F = F - F_0$, in which F_0 represents the fluorescence intensity in the absence of the target DNA, and F is the fluorescence intensity in the presence of the

target), was calculated at each target DNA concentration. The plot of the ΔF value versus the logarithm value of target DNA concentration showed a linear calibration in the range from $c = 50$ to 1600 nM (Figure 4B). The limit of detection (LOD) for target DNA was 10.4 nM, calculated according to the 3 sd/m criterion, in which m is the slope for the range of linearity used and sd is the standard deviation of a blank ($n = 11$, $R = 0.9985$). These results showed that the one-pot synthesized DNA–CdTe QDs can be applied in a biosensing platform based on the ss/dsDNA discrimination of graphene.

In conclusion, DNA–CdTe QDs with excellent properties were prepared by a one-pot method. For the first time, we showed that these QDs can be used in a biosensor for the detection of target HBV DNA, because graphene has different affinities toward ssDNA and dsDNA. Our observations are significant for the following reasons: 1) this work might enrich the FRET technique; 2) it is anticipated that the DNA-functionalized QDs may be applied for the detection of other target molecules, such as proteins based on aptamer recognition and multiplexed DNA; and 3) the QDs can be readily synthesized in a simple and convenient approach, which reduces the cost for analytical detection.

Experimental Section

Preparation of DNA–CdTe QDs: The preparation of DNA–CdTe nanocrystals by a one-step route has been already described in the following experiment.[6] $NaBH_4$ was allowed to react with tellurium powder at a molar ratio of 2:1 in deionized water to produce NaHTe. This process was continued for about 5 h. $CdCl_2$ (1.25 mM) and GSH (1.4 mM) were dissolved in deionized water (10 mL) in an ice-water bath. The solution was adjusted to pH 9.0 by dropwise addition of NaOH solution (1.0 M). Then, an oxygen-free solution containing fresh NaHTe (0.8 μL) was added to the above-mentioned solution (400 μL) in an Eppendorf tube (2 mL), and then a DNA solution containing nucleotides (300 nM) was added. The reaction was conducted at 100 °C for 1 h and then gradually cooled to RT. The mixture was purified by ultrafiltration by using an Amicon Ultra-4 centrifugal-filter device with a MW cutoff of 30 kDa (Millipore Corp.) at 4 °C. Finally, the purified products were collected and stored at 4 °C for further use. Quantum yields (QYs) were measured by using rhodamine 6G (Sigma) in ethanol as the reference standard (QY = 95 %).[19]

Synthesis of graphene nanosheets: GO was prepared by a modified Hummers' method. Briefly, H_2SO_4 (conc., 50 mL) was added into a three-neck flask (500 mL) filled with graphite (1 g) and KNO_3 (0.5 g), while being cooled in an ice-water bath. Then, $KMnO_4$ (4 g) was gradually added to the mixture under vigorous stirring followed by heating the reaction flask to 38 °C. The mixture was allowed to stand for 24 h and diluted with deionized water (300 mL) followed by addition of H_2O_2 (5 mL, 30 wt %) to reduce the insoluble manganese species. Thereafter, the suspension was centrifuged and washed with deionized water a few times, and the resulting solution was dialyzed to purify the product. Finally, the dialysate was treated with ultrasonic exfoliation and then lyophilized to obtain a fluffy GO powder. Graphene sheets were prepared by annealing GO in a home-made tube furnace under high-purity argon. GO was placed in the center of a tube furnace under a flow of argon and then heated at 600 °C for 2 h. After that the product was cooled to RT under continuous flow of argon, which led to the final black sample.

Sensing procedure for HBV DNA: In a typical hybridization procedure, different concentrations of target HBV ssDNA were added to DNA–CdTe (25 nM), and the mixtures were incubated for 20 min, then graphene (3.75 $\mu g\,mL^{-1}$) was added to the above-mentioned mixtures and incubated for 5 min before measurement. Fluorescence emission spectra of the QDs were recorded under excitation at $\lambda = 350$ nm.

Acknowledgements

The authors are very grateful to Professor Shengli Chen's group for generous offer of graphene. This work was financially supported by the National Key Scientific Program Nanoscience and Nanotechnology (Grant no. 2011CB933600), the National Science Foundation of China (Grant no. 21075093) and the Science Fund for Creative Research Groups of NSFC (Grant no. 20921062).

Keywords: biosensors · DNA · FRET · graphene · quantum dots

[1] a) A. P. Alivisatos, *Science* **1996**, *271*, 933–937; b) M. Bruchez, Jr., M. Moronne, P. Gin, S. Weiss, A. P. Alivisatos, *Science* **1998**, *281*, 2013–2016; c) W. C. W. Chan, S. Nie, *Science* **1998**, *281*, 2016–2018; d) X. H. Gao, Y. Y. Cui, R. M. Levenson, L. W. K. Chung, S. M. Nie, *Nat. Biotechnol.* **2004**, *22*, 969–976; e) D. M. Willard, L. L. Carillo, J. Jung, A. Van Orden, *Nano Lett.* **2001**, *1*, 469–474; f) D. Zhao, W. H. Chan, Z. K. He, T. Qiu, *Anal. Chem.* **2009**, *81*, 3537–3543.

[2] a) A. R. Clapp, I. L. Medintz, J. M. Mauro, B. R. Fisher, M. G. Bawendi, H. Mattoussi, *J. Am. Chem. Soc.* **2004**, *126*, 301–310; b) I. L. Medintz, S. A. Trammell, H. Mattoussi, J. M. Mauro, *J. Am. Chem. Soc.* **2004**, *126*, 30–31; c) E. R. Goldman, I. L. Medintz, J. L. Whitley, A. Hayhurst, A. R. Clapp, H. T. Uyeda, J. R. Deschamps, M. E. Lassman, H. Mattoussi, *J. Am. Chem. Soc.* **2005**, *127*, 6744–6751.

[3] a) E. Oh, M. Y. Hong, D. Lee, S. H. Nam, H. C. Yoon, H. S. Kim, *J. Am. Chem. Soc.* **2005**, *127*, 3270–3271; b) L. Z. Liu, H. Li, T. Qiu, G. H. Zhou, K. Y. Wong, Z. K. He, Z. H. Liu, *Chem. Commun.* **2011**, *47*, 2622–2624.

[4] S. P. Wang, N. Mamedova, N. A. Kotov, W. Chen, J. Studer, *Nano Lett.* **2002**, *2*, 817–822.

[5] D. Zhou, J. D. Piper, C. Abell, D. Klenerman, D.-J. Kang, L. Ying, *Chem. Commun.* **2005**, 4807–4809.

[6] N. Ma, E. H. Sargent, S. O. Kelley, *Nat. Nanotechnol.* **2009**, *4*, 121–125.

[7] S. J. Guo, S. J. Dong, *Chem. Soc. Rev.* **2011**, *40*, 2644–2672.

[8] a) H. X. Chang, L. H. Tang, Y. Wang, J. H. Jiang, J. H. Li, *Anal. Chem.* **2010**, *82*, 2341–2346; b) H. Jang, Y. K. Kim, H. M. Kwon, W. S. Yeo, D. E. Kim, D. H. Min, *Angew. Chem.* **2010**, *122*, 5839–5843; *Angew. Chem. Int. Ed.* **2010**, *49*, 5703–5707; c) C. L. Zhang, Y. X. Yuan, S. M. Zhang, Y. H. Wang, Z. H. Liu, *Angew. Chem.* **2011**, *123*, 6983–6986; *Angew. Chem. Int. Ed.* **2011**, *50*, 6851–6854.

[9] a) R. S. Swathi, K. L. Sebastian, *J. Chem. Phys.* **2008**, *129*, 054703; b) R. S. Swathi, K. L. Sebastian, *J. Chem. Phys.* **2009**, *130*, 086101.

[10] a) A. K. Geim, K. S. Novoselov, *Nat. Mater.* **2007**, *6*, 183–191; b) K. S. Novoselov, D. Jiang, F. Schedin, T. J. Booth, V. V. Khotkevich, S. V. Morozov, A. K. Geim, *Proc. Natl. Acad. Sci. USA* **2005**, *102*, 10451–10453.

[11] V. L. Pecoraro, J. D. Hermes, W. W. Cleland, *Biochemistry* **1984**, *23*, 5262–5271.

[12] a) N. Varghese, U. Mogera, A. Govindaraj, A. Das, P. K. Maiti, A. K. Sood, C. N. R. Rao, *ChemPhysChem* **2009**, *10*, 206–210; b) Z. Liu, J. T. Robinson, X. Sun, H. Dai, *J. Am. Chem. Soc.* **2008**, *130*, 10876–10877; c) H. F. Dong, W. C. Gao, F. Yan, H. X. Ji, H. X. Ju, *Anal. Chem.* **2010**, *82*, 5511–5517.

[13] a) H. X. Li, L. Rothberg, *J. Am. Chem. Soc.* **2004**, *126*, 10958–10961; b) H. X. Li, L. Rothberg, *Proc. Natl. Acad. Sci. USA* **2004**, *101*, 14036–14039.

[14] a) M. Lotya, Y. Hemandez, P. J. King, R. J. Smith, V. Nicolosi, L. S. Karlsson, F. M. Blighe, S. De, Z. M. Wang, I. T. McGovern, G. S. Duesberg, J. N. Coleman, *J. Am. Chem. Soc.* **2009**, *131*, 3611–3620; b) M. Lotya, P. J. King, U. Khan, S. De, J. N. Coleman, *ACS Nano* **2010**, *4*, 3155–3162.
[15] L. Tang, Y. Wang, Y. Li, H. Feng, J. Lu, J. H. Li, *Adv. Funct. Mater.* **2009**, *19*, 2782–2789.
[16] S. Stankovich, D. A. Dikin, R. D. Piner, K. A. Kohlhaas, A. Kleinhammes, Y. Jia, Y. Wu, S. T. Nguyen, R. S. Ruoff, *Carbon* **2007**, *45*, 1558–1565.
[17] W. W. Yu, L. H. Qu, W. Z. Guo, X. G. Peng, *Chem. Mater.* **2003**, *15*, 2854–2860.
[18] S. I. Stoeva, J. S. Lee, C. S. Thaxton, C. A. Mirkin, *Angew. Chem.* **2006**, *118*, 3381–3384; *Angew. Chem. Int. Ed.* **2006**, *45*, 3303–3306.
[19] M. Grabolle, M. Spieles, V. Lesnyak, N. Gaponik, A. Eychmüller, U. Resch-Genger, *Anal. Chem.* **2009**, *81*, 6285–6294.

Received: January 11, 2012
Published online: May 31, 2012

